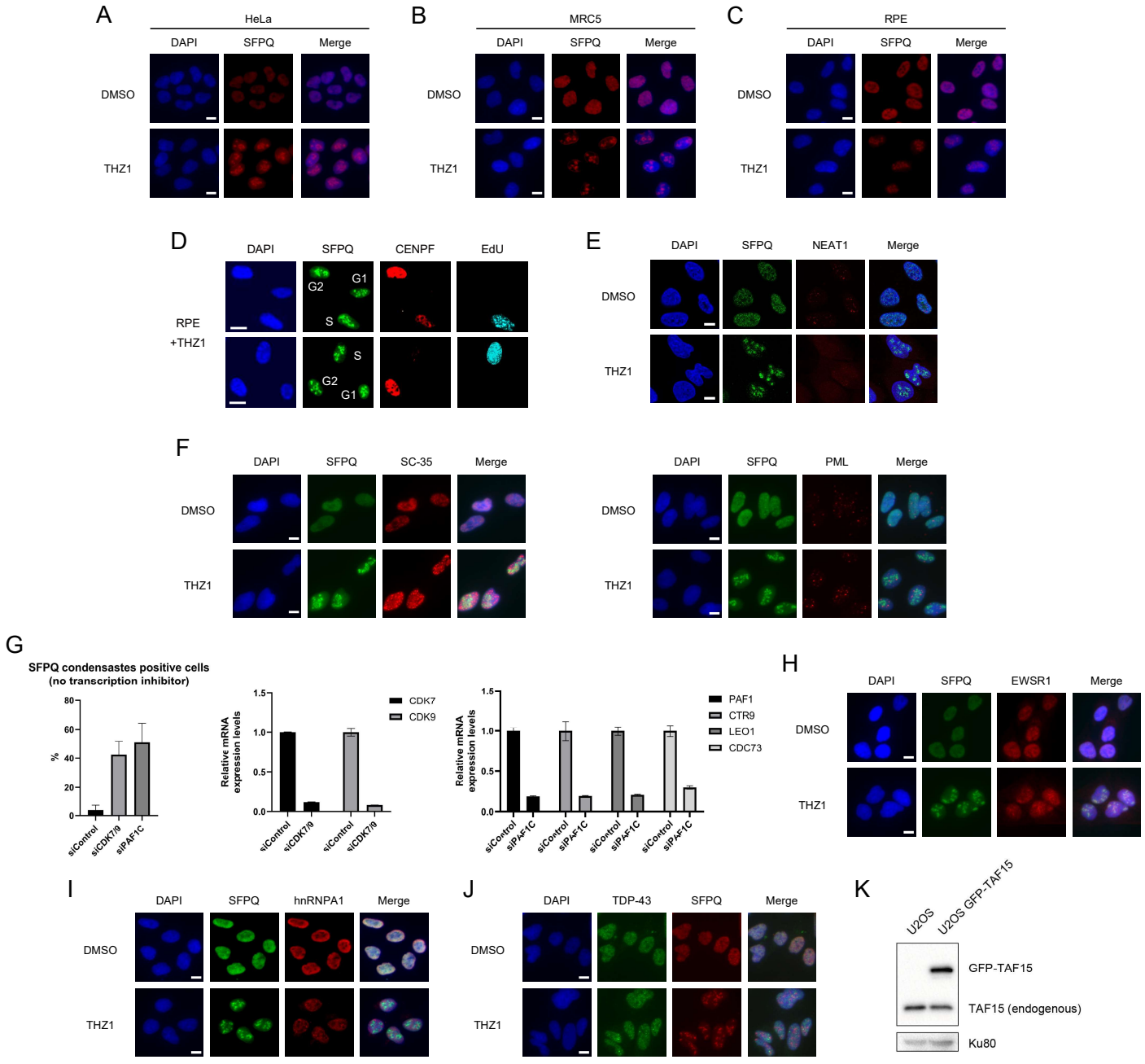

Figure S1. Localization of Paraspeckle Components and the RNA-Binding Proteins after RNAPII Inhibition, related to Figure 1.

(A-C) The effect of THZ1 treatment for 1 hr on the localization of SFPQ was analyzed by IF in the HeLa (A), MRC5 (B), and RPE (C) cell lines. Scale bars, 10 μm.

(D) The CITI formation was analyzed in various cell cycle stage in RPE cells. It is of note that S-phase cells were identified as positive for both CENPF and EdU, G2 cells as CENPF-positive but EdU-negative, and G1 cells as negative for both CENPF and EdU.

(E) NEAT1 localization after THZ1 treatment for 1 hr was examined by RNA FISH for NEAT1. Scale bars, 10 μm.

(F) The effect of THZ1 treatment on the localization of SC-35 (SRSF2) and PML was analyzed by IF. Scale bars, 10 μm.

(G) CITI positive cells were quantified in CDK7/9 or PAF1C KD cells. The KD of CDK7/9 or PAF1C was confirmed by RT-qPCR.

(H-J) The effect of THZ1 treatment on the localization of EWSR1 (H), hnRNPA1 (I), and TDP-43 (J) was analyzed by IF. Scale bars, 10 μm.

(K) The expression level of GFP-TAF15 in GFP-TAF15 cells was confirmed by western blot.

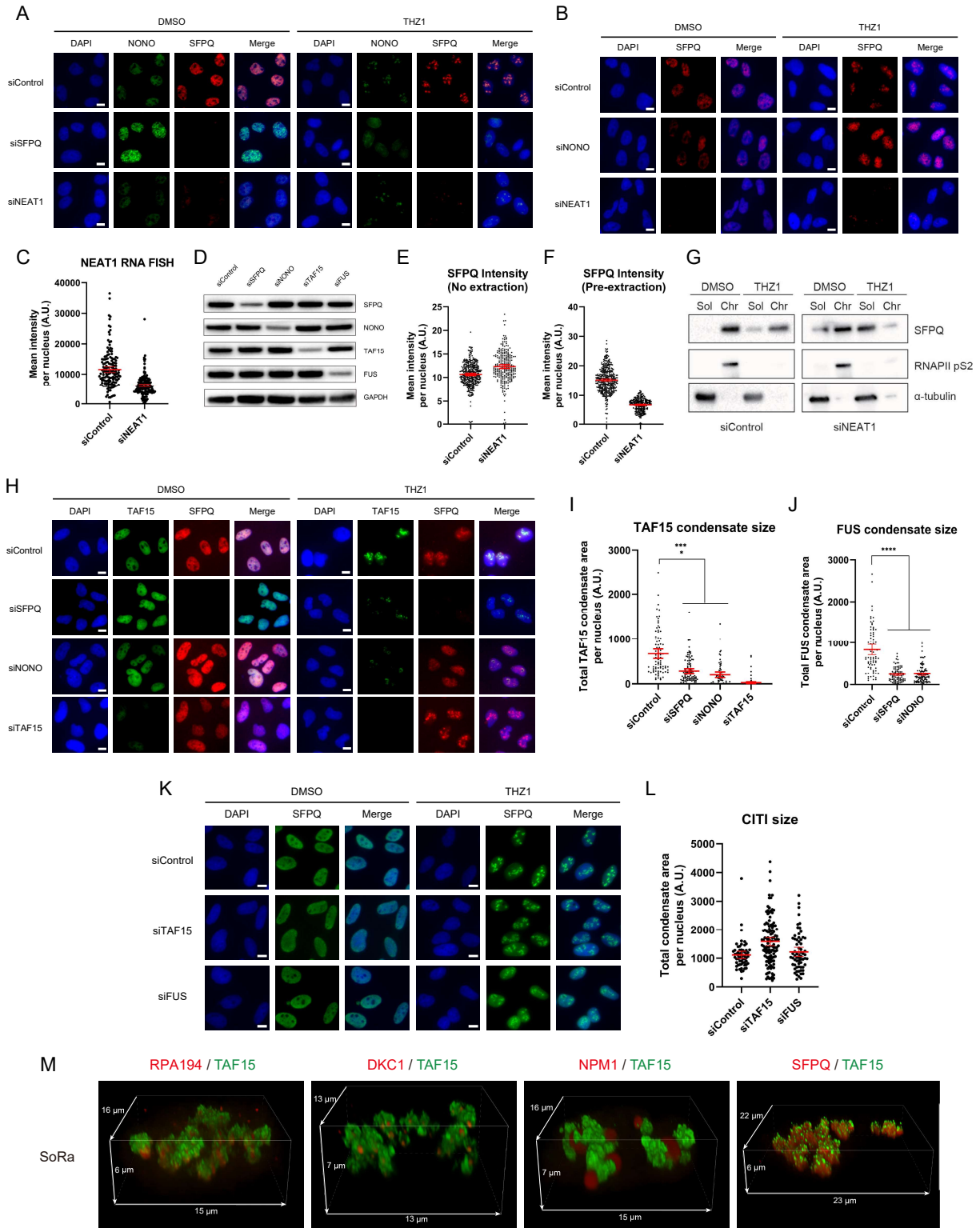

Figure. S2. Functional Relationships of SFPQ/NONO and TAF15/FUS in CITI Formation, related to Figure 1 and 2.

(A, B) The effect of SFPQ, NONO, or NEAT1 KD on the localization of NONO (A) or SFPQ (B) was analyzed by IF. Scale bars, 10 μm.

(C) The efficiency of NEAT1 KD was confirmed by RNA FISH for NEAT1 (mean with 95% CI).

(D) The efficiency of SFPQ, NONO, TAF15, and FUS KD was confirmed by western blot.

(E, F) The SFPQ levels in the nucleus were analyzed by IF with no extraction (E) or extraction (F) before fixation. The pre-extraction resistant signals were considered as the chromatin-bound fraction (mean with 95% CI).

(G) The chromatin binding of SFPQ was analyzed by fractionation western blot. The soluble fraction (Sol) was prepared by extracting cells as in (F). Remaining attached cells were further lysed to prepare the chromatin-bound fraction (Chr).

(H) The effect of SFPQ, or NONO KD on the localization of TAF15 was analyzed by IF. Scale bars, 10 μm.

(I, J) The quantification of the total area of the TAF15 (I) or FUS (J) speckles in SFPQ or NONO KD cells is shown as mean with 95 % CI.

(K, L) The effect of TAF15 or FUS KD on CITIs was analyzed by IF (K). Scale bars, 10 μm. The quantification of the total area of CITIs per cell is shown (L).

(M) The 2-color 3-D SoRa images for the indicated combination.

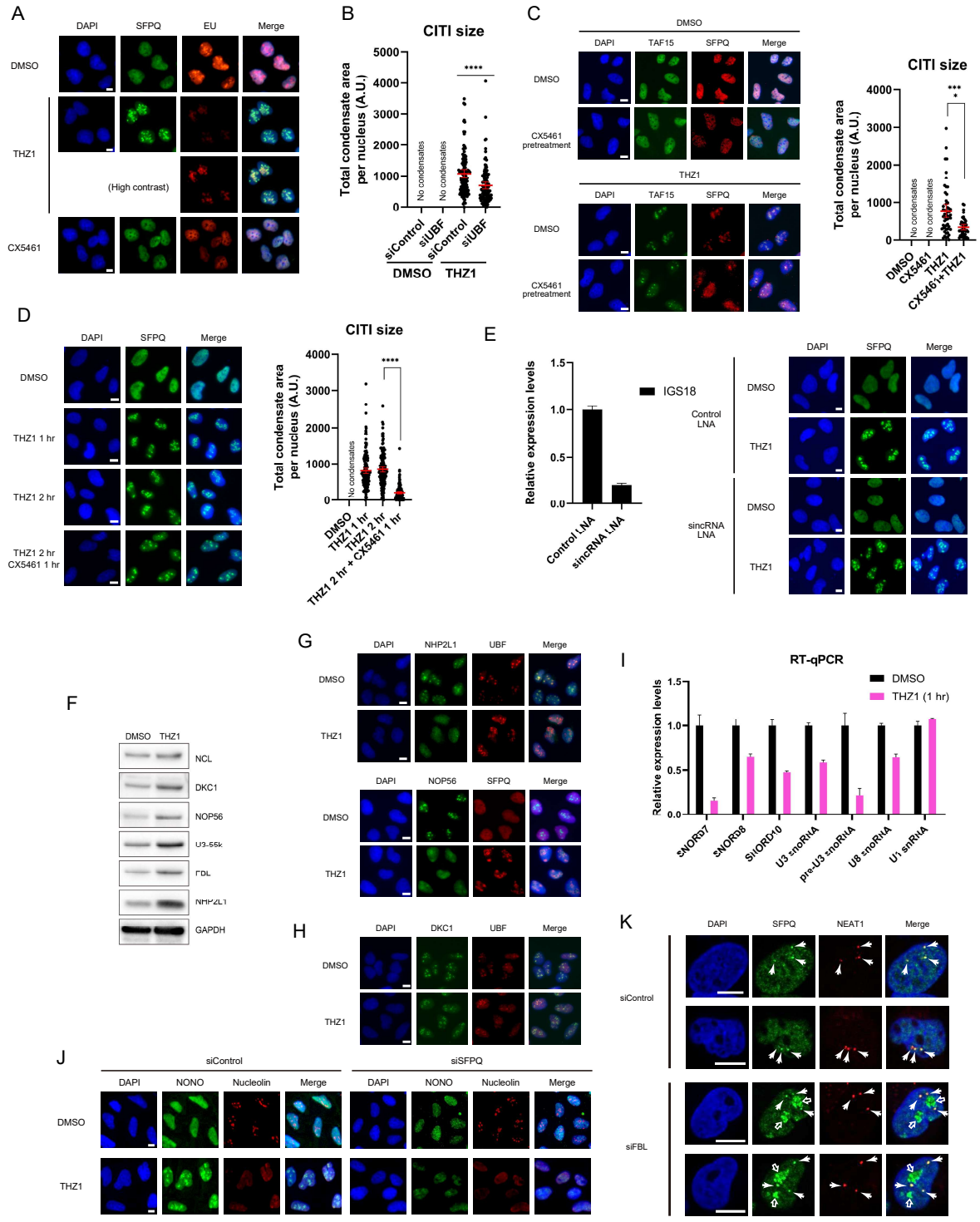

Figure S3. The Box B/C, but not H/ACA snoRNPs are Depleted from Nucleoli upon RNAPII Inhibition, related to Figure 4.

(A) The effect of THZ1 treatment on RNA synthesis at CITI regions was analyzed by visualizing incorporated EU. Scale bars, 10 μm. CX5461 was used as negative control for EU incorporation at nucleoli. The high contrast images for the EU signal of THZ1-treated cells are shown below.

(B) The quantification of the total area of CITIs in UBF KD cells is shown as mean with 95% CI.

(C, D) The effect of pretreatment (C) or posttreatment (D) with CX5461 (1 μM, 24 hr or 10 μM, 1 hr, respectively) on THZ1-induced CITI formation was analyzed by IF. It is of note that CITIs were identified by TAF15 in (C). Scale bars, 10 μm. The quantification of the total area of CITIs per cell is shown as mean with 95% CI.

(E) The effect of sincRNA KD by locked nucleic acid (LNA) oligos on the CITI formation was analyzed by IF. Scale bars, 10 μm. The KD of sincRNA was confirmed by RT-qPCR.

(F) The levels of NCL, DKC1, NOP56, U3-55K, FBL, and NHP2L1 after THZ1 treatment were analyzed by western blot.

(G, H) The effect of THZ1 treatment for 1 hr on the localization of NHP2L1, NOP56 (G), or DKC1 (H) was analyzed by IF. Scale bars, 10 μm.

(I) The levels of snoRNAs were quantified by RT-qPCR.

(J) The effect of SFPQ KD on the depletion of Nucleolin upon THZ1 treatment was analyzed by IF. Scale bars, 10 μm.

(K) The effect of CITI formation on paraspeckles was analyzed in FBL KD cells. Scale bars, 10 μm. CITIs and paraspeckles identified by NEAT1/SFPQ are indicated by open and closed arrows, respectively.

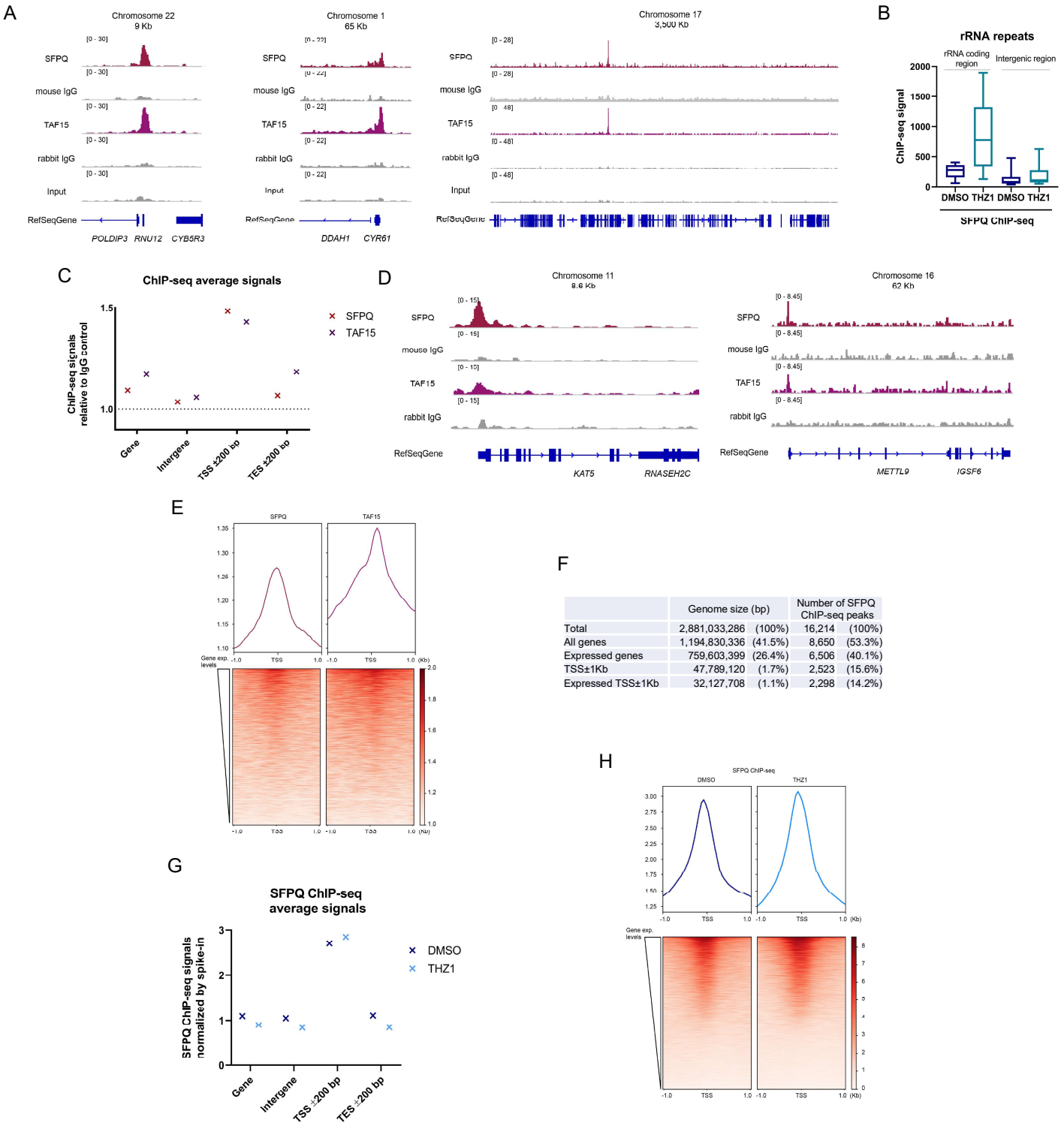

	Genome size (bp)		Number of SFPQ ChIP-seq peaks	
Total	2,881,033,286	(100%)	16,214	(100%)
All genes	1,194,830,336	(41.5%)	8,650	(53.3%)
Expressed genes	759,603,399	(26.4%)	6,506	(40.1%)
TSS±1Kb	47,789,120	(1.7%)	2,523	(15.6%)
Expressed TSS±1Kb	32,127,708	(1.1%)	2,298	(14.2%)

Figure S4. Association of SFPQ/TAF15 with TSSs of Genes, related to Figure 5.

(A) Representative peaks of SFPQ/TAF15 ChIP-seq are shown in various scales. The samples from IgG control and Input as well as RefSeqGene are aligned.

(B) SFPQ ChIP-seq signals were quantified at the rRNA coding region and intergenic region in rDNA repeats.

(C) The binding sites of SFPQ/ TAF15 within gene regions were analyzed by ChIP-seq. The average signals relative to IgG control within each category of regions were plotted. TES, transcription end site.

(D, E) The correlation between the binding of SFPQ/TAF15 to TSSs ± 1 Kb and gene expression levels was analyzed by ChIP-seq. The tracks from two representative genes are shown in (D). The average signals relative to IgG control for all genes expressed at any level are shown in upper panels in (E). In the heatmaps below, genes are sorted dependent on their expression levels defined by RNA-seq.

(F) The number of SFPQ ChIP-seq peaks determined from two biological replicates was analyzed in the indicated genomic regions.

(G) The binding sites of SFPQ/TAF15 within gene regions were analyzed by ChIP-seq normalized by spike-in control as in (C).

(H) The correlation between the binding of SFPQ/TAF15 to TSSs ± 1 Kb and gene expression levels was analyzed by ChIP-seq normalized by spike-in control as in (E).

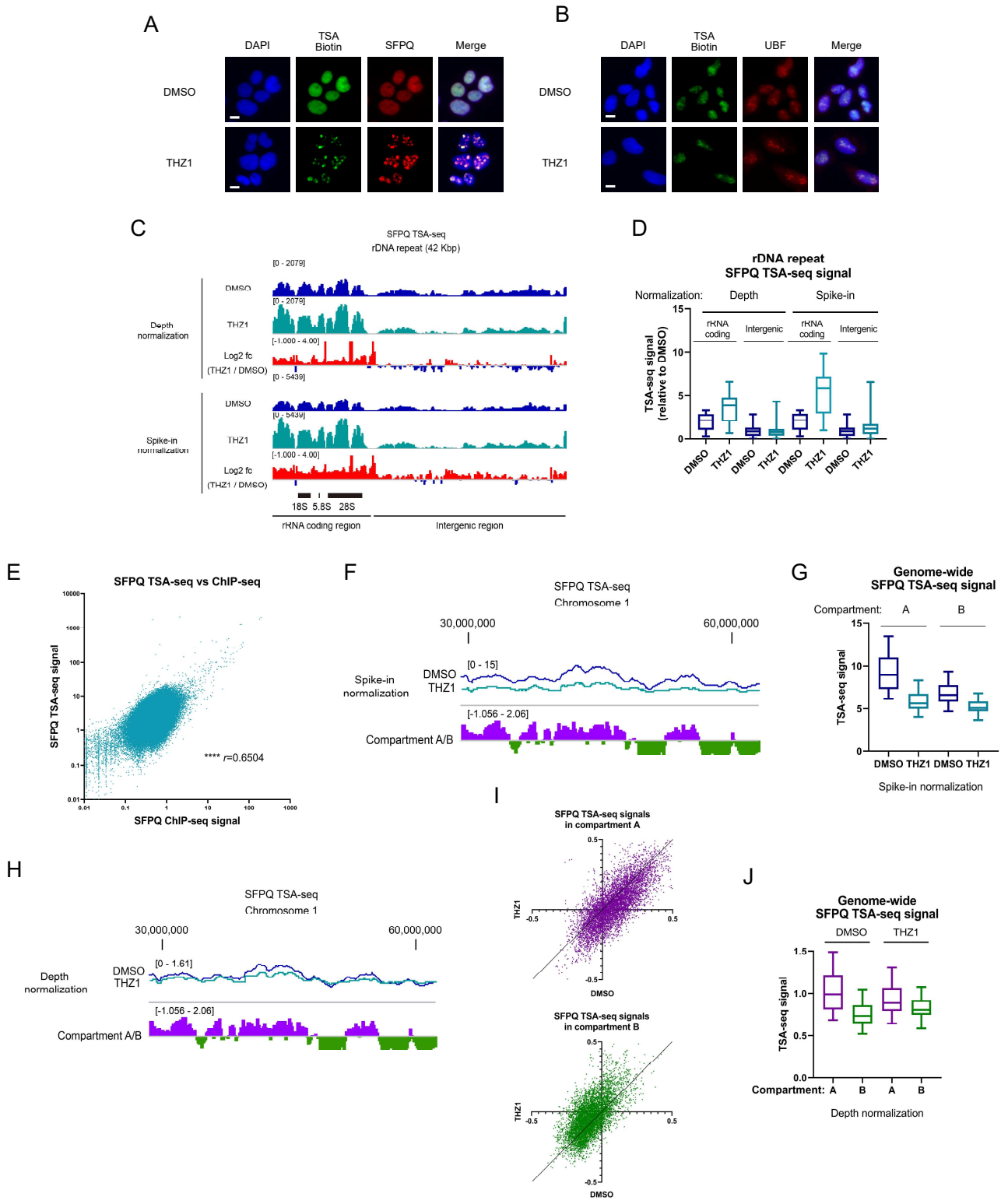

Figure S5. SFPQ Remains Associated with Compartment A after THZ1 Treatment, related to Figure 5.

(A, B) Representative images for TSA labelling of SFPQ (A) or UBF (B) using the TSA-seq protocol.

(C, D) The effect of depth normalization and spike-in normalization on SFPQ TSA-seq signals were compared in the rDNA repeat unit (C). The quantification of signals within each category of regions is shown as in Figure 5C (D).

(E) The SFPQ ChIP-seq and TSA-seq signals were analyzed with the scatter plot (Pearson's correlation coefficient, *r*=0.6504).

(F, G) Representative genomic view of SFPQ TSA-seq normalized by spike-in control is shown (F). The signals within each compartment are shown as a box plot (G).

(H-J) Representative genomic view of SFPQ TSA-seq normalized by sequencing depth is shown (H). The signals within each compartment are shown as a scatter plot (I) or a box plot (J).

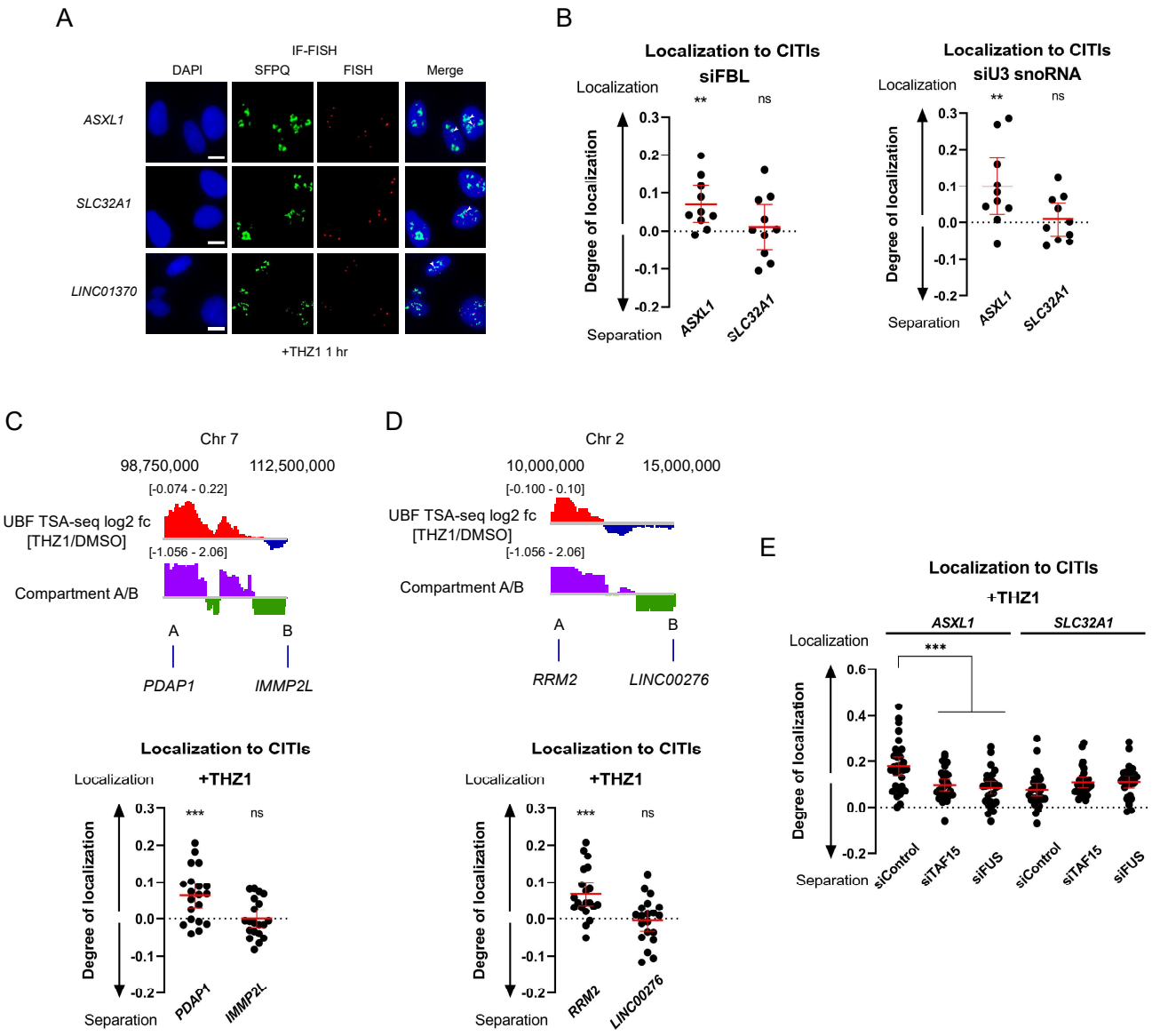

Figure S6. The Genes in Compartment A Associate with CITIs, related to Figure 5.

(A) Representative images for the IF-FISH analysis. Scale bars, 10 μm. Colocalization between FISH signal and CITIs is indicated by white arrows.

(B) The colocalization frequency of the FISH signal and CITIs was analyzed in FBL or U3 snoRNA KD cells.

(C, D) Colocalization between the gene loci on Chr 7 (C) or Chr 2 (D) and CITIs was analyzed by FISH as in (B). The log2 ratio of UBF TSA-seq signals (THZ1/DMSO) and compartment A/B prediction scores at each locus are shown above.

(E) The effect of TAF15 or FUS KD on the colocalization frequency of the FISH signal and CITIs was analyzed in THZ1-treated cells (mean with 95% CI, *n*=30 for data points from three biological replicates).

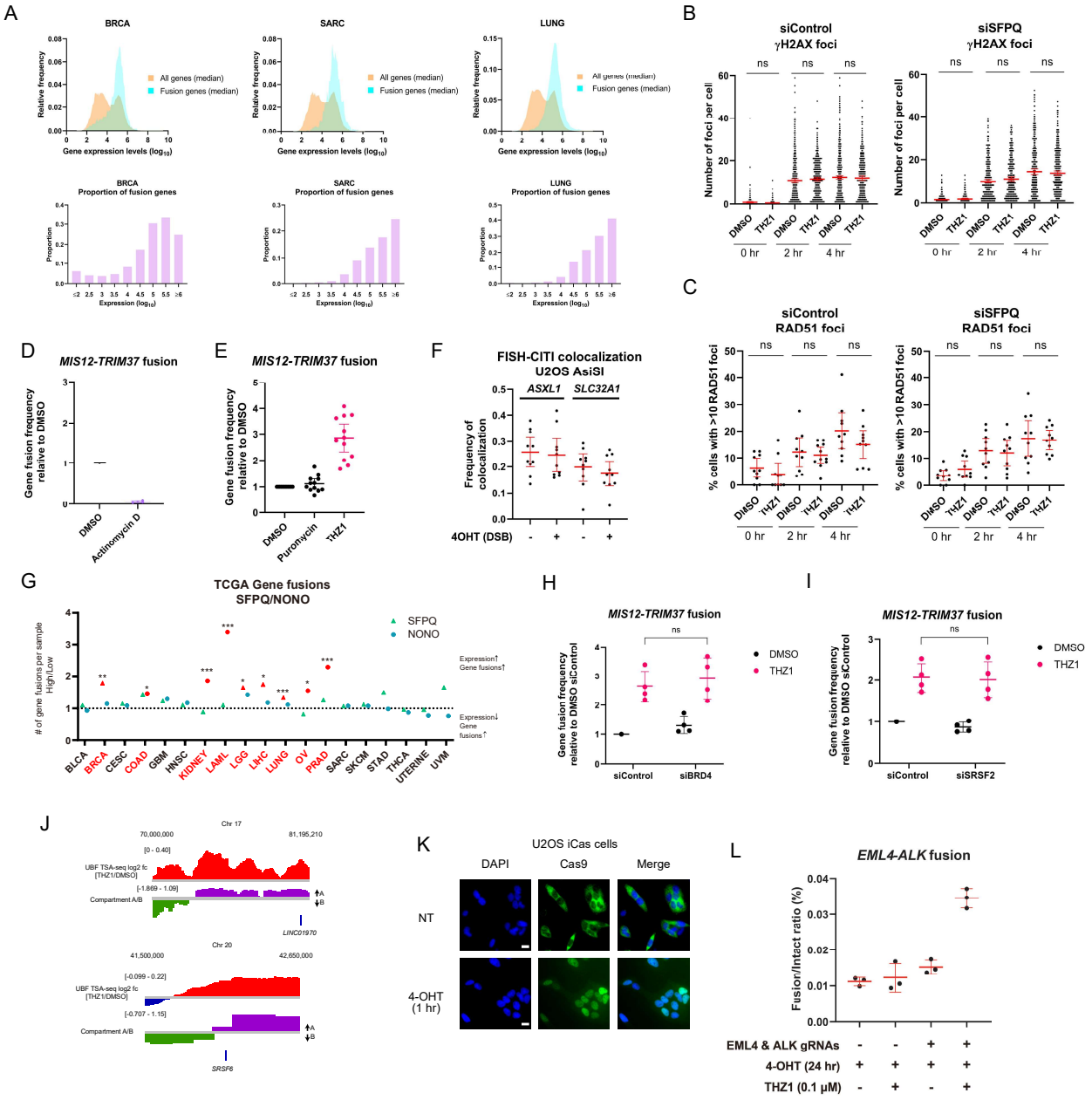

Figure S7. Highly Transcribed Genes Have a Higher Risk of Gene Fusion in Cancer, related to Figure 6 and 7.

(A) The distribution of the expression levels of all genes or a set of genes that underwent fusions (fusion genes) in TCGA samples was analyzed. The proportion of the fusion genes in each expression bin is also shown below.

(B) The number of γH2AX foci per cell was measured at the indicated time points after 4-OHT treatment.

(C) The percentage of cells that have more than 10 RAD51 foci was measured at the indicated time points after 4-OHT treatment.

(D) The effect of Actinomycin D treatment on the frequency of *MIS12-TRIM37* fusion was analyzed (mean with SD, *n*=4 for data points from one representative experiment of three biological replicates).

(E) The effect of Puromycin treatment on the frequency of *MIS12-TRIM37* fusion was analyzed (mean with 95% CI, *n*=12 for data points from three biological replicates).

(F) The effect of DSB induction on the colocalization frequency of the FISH signal of *ASXL1* or *SLC32A1* and CITIs was analyzed in the THZ1-treated U2OS AsiSI cells (mean with 95% CI, *n*=10 for data points from one representative experiment of three biological replicates).

(G) The correlation between the SFPQ or NONO expression levels and the number of gene fusions per sample was analyzed in the indicated TCGA datasets as in Figure 6A. See also Table S2.

(H, I) The effect of BRD4 KD (H) or SRSF2 KD (I) on the frequency of *MIS12-TRIM37* fusion was analyzed (mean with SD, *n*=4 for data points from one representative experiment of three biological replicates).

(J) The position of *LINC01970* on Chr 17 and *SRSF6* on Chr 20 and the log2 ratio of UBF TSA-seq signals (THZ1/DMSO) and compartment A/B scores at these loci are shown.

(K) The nuclear import of ER-Cas9 after 4-OHT treatment (1 hr) in U2OS iCas cell line was confirmed by IF. Scale bars, 5 μm.

(L) The effect of THZ1 treatment on the frequency of *EML4-ALK* fusion was analyzed by qPCR in the cells transfected with the indicated gRNAs and treated as indicated (mean with SD, *n*=3 from one representative experiment of three biological replicates).

Table S1. Metrics for Sequencing Experiments in This Study, related to Figure 4, S4, and S5.

Cell	Experiment	Target	Treatment	Genome	Number of total reads	Number of mapped reads	FDR 0.01 peaks	FDR 0.05 peaks	5-fold enrichment peaks
U2OS	ChIP-seq	SFPQ	DMSO	hg19	20,942,233	20,140,663	37,637	12,252	11,852
U2OS	ChIP-seq	SFPQ	DMSO (Spike-in)	hg19	17,752,137	15,184,154	20,096	6,083	8,697
U2OS	ChIP-seq	SFPQ	DMSO (Spike-in)	rDNA repeats	19,313,925	164,836	-	-	-
U2OS	ChIP-seq	SFPQ	THZ1	hg19	23,720,092	22,965,250	55,329	16,885	11,760
U2OS	ChIP-seq	SFPQ	THZ1 (Spike-in)	hg19	19,597,622	16,218,603	38,234	8,793	10,101
U2OS	ChIP-seq	SFPQ	THZ1 (Spike-in)	rDNA repeats	21,338,700	275,900	-	-	-
U2OS	ChIP-seq	TAF15	DMSO	hg19	19,454,100	18,760,462	2,462	956	992
U2OS	ChIP-seq	TAF15	DMSO (Spike-in)	hg19	19,572,788	18,254,768	3,519	1,218	1,376
U2OS	ChIP-seq	TAF15	THZ1	hg19	22,531,125	21,780,270	12,724	1,266	1,023
U2OS	ChIP-seq	TAF15	THZ1 (Spike-in)	hg19	20,824,653	19,452,442	5,417	1,316	1,572
U2OS	ChIP-seq	Input	DMSO (Spike-in)	hg19	21,612,257	20,721,987	1,660	1,095	1,025
U2OS	ChIP-seq	Input	THZ1 (Spike-in)	hg19	21,579,067	20,752,745	1,745	1,131	1,052
U2OS	ChIP-seq	Mouse IgG	DMSO (Spike-in)	hg19	14,090,300	12,165,017	1,760	1,078	1,133
U2OS	ChIP-seq	Mouse IgG	THZ1 (Spike-in)	hg19	19,949,410	17,907,191	1,682	1,194	1,136
U2OS	ChIP-seq	Rabbit IgG	DMSO (Spike-in)	hg19	18,390,936	16,969,037	1,743	1,171	1,128
U2OS	ChIP-seq	Rabbit IgG	THZ1 (Spike-in)	hg19	14,754,651	12,121,073	2,071	1,258	1,326
U2OS	TSA-seq	UBF	DMSO	hg19	38,998,920	14,428,090	-	-	-
U2OS	TSA-seq	UBF	THZ1	hg19	36,237,106	13,610,763	-	-	-
U2OS	TSA-seq	UBF	DMSO-siControl	hg19	35,104,424	13,992,880	-	-	-
U2OS	TSA-seq	UBF	THZ1-siControl	hg19	39,735,796	19,579,843	-	-	-
U2OS	TSA-seq	UBF	DMSO-siTAF15	hg19	48,416,368	20,746,599	-	-	-
U2OS	TSA-seq	UBF	THZ1-siTAF15	hg19	47,445,916	16,105,781	-	-	-
U2OS	TSA-seq	SFPQ	DMSO	hg19	45,019,420	23,271,398	-	-	-
U2OS	TSA-seq	SFPQ	DMSO	rDNA repeats	45,019,420	202,555	-	-	-
U2OS	TSA-seq	Input	DMSO	hg19	33,450,584	32,881,545	-	-	-
U2OS	TSA-seq	Input	DMSO	rDNA repeats	33,450,584	175,228	-	-	-
U2OS	TSA-seq	SFPQ	THZ1	hg19	41,959,368	11,701,143	-	-	-
U2OS	TSA-seq	SFPQ	THZ1	rDNA repeats	41,959,368	108,492	-	-	-
U2OS	TSA-seq	Input	THZ1	hg19	39,110,846	38,421,634	-	-	-
U2OS	TSA-seq	Input	THZ1	rDNA repeats	39,110,846	207,978	-	-	-
U2OS	TSA-seq	SFPQ	DMSO (Spike-in)	hg19	211,804,024	97,117,947	-	-	-
U2OS	TSA-seq	SFPQ	DMSO (Spike-in)	rDNA repeats	211,804,024	334,915	-	-	-
U2OS	TSA-seq	Input	DMSO (Spike-in)	hg19	113,170,426	106,281,768	-	-	-
U2OS	TSA-seq	Input	DMSO (Spike-in)	rDNA repeats	113,170,426	384,073	-	-	-
U2OS	TSA-seq	SFPQ	THZ1 (Spike-in)	hg19	211,078,626	63,231,373	-	-	-
U2OS	TSA-seq	SFPQ	THZ1 (Spike-in)	rDNA repeats	211,078,626	390,548	-	-	-
U2OS	TSA-seq	Input	THZ1 (Spike-in)	hg19	82,577,772	72,041,017	-	-	-
U2OS	TSA-seq	Input	THZ1 (Spike-in)	rDNA repeats	82,577,772	460,541	-	-	-

Table S2. The Original TCGA Analysis Data, related to Figure 6 and S7.

For Figure 6A:

Genes	Study	Low group			High group			*P* value
		Fusion #	SD	*N*	Fusion #	SD	*N*	
CDK7	BRCA	4.59	5.79	490	3.41	4.47	619	0.000209***
	SARC	8.07	10.12	95	5.93	6.81	164	0.0676
	LUNG	2.92	3.86	436	2.70	2.97	650	0.308
CDK9	BRCA	5.15	6.44	341	3.39	4.32	768	4.62E-06***
	SARC	8.08	9.37	112	5.68	7.10	147	0.0245*
	LUNG	2.99	3.21	247	2.73	3.39	839	0.259
TFIIS	BRCA	4.83	6.19	171	3.37	4.03	294	0.00603**
	SARC	7.24	7.85	63	3.60	5.01	45	0.00409**
	LUNG	2.66	2.83	238	2.97	3.56	243	0.282
PAF1C	BRCA	4.64	5.96	377	3.03	4.10	195	1.55E-04***
	SARC	7.76	9.00	50	6.02	7.12	58	0.272
	LUNG	2.65	2.67	138	2.94	3.86	450	0.316
NELF	BRCA	2.02	2.80	90	3.79	4.39	304	8.51E-06***
	SARC	4.20	6.66	15	6.42	7.15	88	0.240
	LUNG	2.37	2.43	139	3.93	5.39	158	0.00114**
DSIF+SPT6	BRCA	3.11	4.33	80	4.43	5.18	233	0.0274*
	SARC	8.59	8.60	41	6.37	8.16	214	0.0736
	LUNG	2.52	2.92	366	2.92	3.55	720	0.0485*

.

TFIIS: TCEA1, TCEA2
PAF1C: PAF1, LEO1, RTF1, CDC73, CTR9
NELF: NELFA, NELFB, NELFCD, NELFE
DSIF: SUPT4H1, SUPT5H
BRCA: breast invasive carcinoma
SARC: sarcoma
LUNG: lung adenocarcinoma and squamous cell carcinoma

Table S2 (Continued)

For Figure S7G:

Genes	Study	Low group			High group			*P* value
		Fusion #	SD	*N*	Fusion #	SD	*N*	
SFPQ	BLCA	2.58	3.53	60	2.84	3.44	354	0.595
	BRCA	2.25	3.17	83	4.02	5.13	1026	0.00241**
	CESC	1.34	2.04	29	1.55	2.15	277	0.604
	COAD	0.49	1.01	63	0.70	1.18	458	0.130
	GBM	1.58	1.67	79	1.96	3.37	90	0.354
	HNSC	1.32	1.36	69	1.46	1.63	433	0.430
	KIDNEY	0.61	1.93	264	0.54	1.29	627	0.606
	LAML	0.67	1.00	9	0.74	1.16	142	0.834
	LGG	1.30	3.08	252	2.14	4.62	276	0.0135*
	LIHC	1.43	2.29	47	2.49	4.95	327	0.0142*
	LUNG	2.21	2.51	247	2.96	3.55	839	2.25E-04***
	OV	1.13	2.03	23	0.92	1.62	356	0.633
	PRAD	2.85	3.60	26	3.59	3.69	472	0.308
	SARC	6.36	7.97	47	6.80	8.30	212	0.737
	SKCM	2.33	3.35	52	2.61	3.84	418	0.575
	STAD	1.26	3.32	31	1.88	4.42	344	0.332
	THCA	0.39	0.68	66	0.38	0.68	444	0.862
	UTERINE	5.11	8.22	19	4.89	6.75	229	0.910
	UVM	0.25	0.45	12	0.41	1.40	68	0.451

Genes	Study	Low group			High group			*P* value
		Fusion #	SD	*N*	Fusion #	SD	*N*	
NONO	BLCA	2.99	4.23	74	2.77	3.26	340	0.675
	BRCA	3.47	5.31	126	3.99	5.10	983	0.300
	CESC	1.43	2.33	47	1.55	2.10	259	0.728
	COAD	0.58	1.11	318	0.84	1.24	203	0.0147*
	GBM	1.42	1.69	24	1.84	2.84	145	0.312
	HNSC	1.26	1.65	85	1.48	1.58	417	0.258
	KIDNEY	0.32	0.61	136	0.60	1.62	755	4.28E-04***
	LAML	0.23	0.44	13	0.78	1.18	138	6.22E-04***
	LGG	1.38	2.11	204	1.96	4.79	324	0.0547
	LIHC	2.08	3.86	106	2.46	5.01	268	0.435
	LUNG	2.60	2.75	438	2.91	3.70	648	0.112
	OV	0.65	1.14	81	1.01	1.76	298	0.0278*
	PRAD	1.59	2.32	22	3.64	3.71	476	1.05E-04***
	SARC	6.46	7.88	130	6.98	8.58	129	0.615
	SKCM	2.42	3.67	99	2.62	3.82	371	0.645
	STAD	1.85	3.31	41	1.83	4.45	334	0.962
	THCA	0.43	0.73	23	0.38	0.68	487	0.713
	UTERINE	5.93	8.87	160	4.60	6.14	447	0.0815
	UVM	0.50	0.55	6	0.38	1.34	74	0.657

Table S2 (Continued)

BLCA: bladder urothelial carcinoma, CESC: cervical squamous cell carcinoma and endocervical adenocarcinoma, COAD: colon adenocarcinoma, GBM: glioblastoma multiforme, HNSC: head and neck squamous cell carcinoma, KIDNEY: kidney chromophobe, renal clear cell carcinoma, and renal papillary cell carcinoma, LAML: acute myeloid leukemia, LGG: brain lower grade glioma, LIHC: liver hepatocellular carcinoma, OV: ovarian serous cystadenocarcinoma, PRAD: prostate adenocarcinoma, SKCM: skin cutaneous melanoma, STAD: stomach adenocarcinoma, THCA: thyroid carcinoma, UTERINE: uterine corpus endometrial carcinoma and carcinosarcoma, UVM: uveal melanoma.

Table S3. Oligonucleotides Used in This Study, related to STAR Methods.

Assay	Oligo name	Sequence (5'-3')	Company
Gene fusion	Chr17-MIS12-F	GAAGCAGTTCCTGCGCTCTG	IDT
	Chr17-MIS12-R	GATTCAACGCAGAGGTGCCC	IDT
	Chr17-TRIM37-F	GGCGAGAGAAGCTGCGAA	IDT
	Chr17-TRIM37-R	CGAGTCGCCAAGTCTCGTAT	IDT
	Chr9-PIP5KL1-F	GCGGCCGACCAATAGCA	IDT
	Chr9-PIP5KL1-R	GCCGGACCGAGGTCTGAAG	IDT
	Chr9-NR6A1-F	TAAATAAATCGGGTTTGCCGCC	IDT
	Chr9-NR6A1-R	AGGAGCTTTTGTGAGGTCGTA	IDT
	Chr9-GNE-F	ACTCGTCGCTCGACCTTGTC	IDT
	Chr9-GNE-R	GACGGGAGCAGCCAATCAC	IDT
	Chr9-LINGO2-F	CAGAAAGTGTGAGGACAGGACA	IDT
	Chr9-LINGO2-R	TAGGAGGATCTCTCCGGGCG	IDT
	Chr20-ASXL1-F	CTCTGACCCCGTGGTTATGC	IDT
	Chr20-ASXL1-R	CGTCAGTCGCCCACGG	IDT
	Chr20-SLC32A1-F	GGGTCCGCAGCATAAGTGT	IDT
	Chr20-SLC32A1-R	GTTTGCGCTCTCACCGCTA	IDT
	Chr13-RASA3-F	CCTGTGGGTCCCTGACTCAT	IDT
	Chr13-RASA3-R	TGCATGACTGAGCCACACTT	IDT
	Chr13-NGR-F	GGAAGACACGTCATCCCCTG	IDT
	Chr13-NGR-R	ACAGCCTATGGGCACATTACAT	IDT
	Chr17-LINC01970-F	GAGTCATGTGCCCGGAGAG	IDT
	Chr17-LINC01970-R	GGATGCGGCCCTAAGACTTG	IDT
	Chr17-SRSF6-F	TGAACGGCAAGGAGCTCTG	IDT
	Chr17-SRSF6-R	GCGGCTTCCGTAGCTGTAG	IDT
	EML4-sgRNA-F	accgGACCTGAACAGCAAGTTTGT	IDT
	EML4-sgRNA-R	aaacACAAACTTGCTGTTCAGGTC	IDT
	ALK-sgRNA-F	accgGGCCTTGCTGAAACTTCCTT	IDT
	ALK-sgRNA-R	aaacAAGGAAGTTTCAGCAAGGCC	IDT
	EML4-F	TCTACCTATGCCAGTGAACACA	IDT
	EML4-R	AATTCAGCAGAGCTGGAAGTAGA	IDT
	ALK-R	ACCCTGGGTGCCATGGAG	IDT
Cloning	TAF15-HindIII-F	TGCAgaattcCTaAtaAggCcTAttCcTTtgGtcGtttctgtagtcgtttcttcctccc	IDT
	TAF15-EcoRI-R	GATTCAACGCAGAGGTGCCC	IDT
	FUS-XhoI-F	AGATCTCGAGCTgcAAGCaaTgattatacccaacaagcaaccca	IDT
	FUS-KpnI-R	GGATCCCGGGCCCGCGGTACCttaatacggcctctccctgcg	IDT
RT-qPCR	SNORD7-F	ATGCGATGATGAGTGAAGTAGAG	IDT
	SNORD7-R	CAGCTCAGAGAGAAGATTAAGAG	IDT
	SNORD8-F	TCCCAATGATGAGTTGCCATGC	IDT
	SNORD8-R	CCCCTCAGATCTTCATGTGAG	IDT
	SNORD10-F	GCTCTGTGATGGAGCCCATG	IDT
	SNORD10-R	TAGTCTGCTCTCAGAGTACAAAGAC	IDT
	U3 snoRNA-F3	AGAGGTAGCGTTTTCTCCTGAGCG	IDT

Table S3 (Continued)

	U3 snoRNA-R3	ACCACTCAGACCGCGTTCTC	IDT
	pre-U3 snoRNA-R1	AAGGAAAAACCACTCAGA	IDT
	pre-U3 snoRNA -R2	AAGGAAAAACCACTCA	IDT
	U8 snoRNA-F	CGTCAGGTGGGATAATCCTT	IDT
	U8 snoRNA-R	GGGTGTTGCAAGTCCTGATT	IDT
	U1-F	CCATGATCACGAAGGTGGTTT	IDT
	U1-R	ATGCAGTCGAGTTTCCCACAT	IDT
	CDK7-F	AAGTCTCGGGCAAAGCG	Sigma-Aldrich
	CDK7-R	AGCTTCTGATCTATGTCCAAGTT	Sigma-Aldrich
	CDK9-F	AATACGAGAAGCTCGCCAAGA	Sigma-Aldrich
	CDK9-R	CTCCCGCAAGGCTGTAATGG	Sigma-Aldrich
	PAF1-F	CATCTTCCGAGAGGGTGACG	Sigma-Aldrich
	PAF1-R	CCCGATGTTTGACCACAAGC	Sigma-Aldrich
	LEO1-F	GGGCATTCGAGAGGAACGAG	Sigma-Aldrich
	LEO1-R	TTCTCTTTCCGGAAGGTTCAC	Sigma-Aldrich
	CTR9-F	CTCCATCGAGATTCCCCTCC	Sigma-Aldrich
	CTR9-R	TTGCCATCTATACGTGCTGCT	Sigma-Aldrich
	CDC73-F	CTGGCCCAAGAATGTGAAGAC	Sigma-Aldrich
	CDC73-R	GCACGTCGGACATAAACAGGAT	Sigma-Aldrich
Knockdown	Control	CGUACGCGGAAUACUUCGAdTdT	Sigma-Aldrich
	SFPQ	GCCAGCAGCAAGAAAGGCAUUUGAAdTdT	Sigma-Aldrich
	SFPQ	GACGACAGGAAGAAUUAAGdTdT	Sigma-Aldrich
	NONO	GGAAGCCAGCUGCUCGGAAAGCUCUdTdT	Sigma-Aldrich
	NEAT1-1	GAGGAGUGAUGUGGAGUUAAG	IDT
	NEAT1-2	GGGAUGAUGCAAACAAUUACU	IDT
	TAF15	UGAUCAGCGCAACCGACCAdTdT	Sigma-Aldrich
	TAF15	GCUCGAAGGAAUUCCTGCAAUdTdT	Thermo Scientific
	FUS	CGGACAUGGCCUCAAACGAdTdT	Sigma-Aldrich
	SRSF2	SMARTpool ON-TARGETplus L-019711-00-0005	Horizon
	BRD4	SMARTpool ON-TARGETplus L-004937-00-0005	Horizon
	Nucleolin	SMARTpool ON-TARGETplus L-003854-00-0005	Horizon
	FBL	SMARTpool ON-TARGETplus L-011269-00-0005	Horizon
	UBF	SMARTpool ON-TARGETplus L-020670-00-0005	Horizon
	U3 (siRNA)	CTGAACGTGTAGAGCACCGAAdTdT	IDT
	SCR-ASO	mUmCmAmCmCTTCACCCTCTmCmCmAmCmU	IDT
	U3-ASO	mUmUmCmGmGTGCTCTACACmGmUmUmCmA	IDT
	U8-ASO	mGmGmAmUmUATCCCACCTGmAmCmGmAmU (mN: 2´-*O*-methoxyethylribonucleotide)	IDT
	CDK7	SMARTpool ON-TARGETplus L-003241-00-0005	Horizon
	CDK9	SMARTpool ON-TARGETplus L-003243-00-0005	Horizon
	PAF1	AAGCAGCAGTTTACCGAGGAA	Sigma-Aldrich
	LEO1	GCCGGUAGCUUCUGAUAAU	Sigma-Aldrich
	CTR9	CCGUGUGGCUCCAAACUUUA	Sigma-Aldrich
	CDC73	GGUACAUGGUAAAGCAUAA	Sigma-Aldrich

Table S3 (Continued)

RNA FISH	NEAT1	Stellaris NEAT1 RNA FISH probes	LGC Biosearch
	U3 snoRNA	GCTCTACACGTTCAGAGAAACTTCTCTAGTAACACACTATAGAA ATGATCC	IDT
DNS FISH	ASXL1	ASXL1-20-RE	Empire Genomics
	SLC32A1	SLC32A1-20-RE	Empire Genomics
	LINC01370	LINC01370-20-RE	Empire Genomics
	Chr20 CEN	CHR20-10-GR	Empire Genomics
	PDAP1	PDAP1-20-RE	Empire Genomics
	IMMP2L	IMMP2L-20-RE	Empire Genomics
	RRM2	RRM2-20-RE	Empire Genomics
	LINC00276	LINC00276-20-RE	Empire Genomics
RIP	pre-rRNA Forward	TGTCAGGCGTTCTCGTCTC	IDT
	pre-rRNA Reverse	AGCACGACGTCACCACATC	IDT
	NEAT1-F	TGACTCTCCATTTCCCCATC	IDT
	NEAT1-R	TCATTTACCCGCATTTCACA	IDT
	GAPDH-F	GGTCTCCTCTGACTTCAACA	IDT
	GAPDH-R	GTGAGGGTCTCTCTCTTCCT	IDT